International Journal of Applied Engineering Research ISSN 0973-4562 Volume 10, Number 14 (2015) pp 34420-34427

Prediction of service life of concrete structure from half-cell potentiometer data – validation based on case study

K.M.Godbole[1], Dr. P.H.Sawant[2], Dr. B.B.Das[3*], J.R. Dhanuskar[4]
Research Scholar, Department of Civil Engineering, Sardar Patel College of Engineering, Andheri, Mumbai, India.
Professor, Department of Civil Engineering, Sardar Patel College of Engineering, Andheri, Mumbai, India.
Sr. Associate Professor, National Institute of Construction Management and Research, Indore, India.
Assistant Professor, Datta Meghe College of Engineering, Airoli, Navi Mumbai.
*Corresponding Author

Abstract- This paper presents a brief review of the models developed by earlier researchers to predict the service life of the reinforced concrete structure with consideration to design, materials, quality control, construction technology, environmental factors and the maintenance/monitoring strategy adopted. In addition, a number of case studies on the concrete structures under marine environment were considered for the life performance assessment through non destructive half-cell potentiometer test data. The results of the remaining service life obtained from the model are compared with the actual field condition and it is found that both are matching appropriately.

Keywords- Concrete, Corrosion, Chloride, Cracking, Service Life Model

1. Introduction

The service life of a structure can be defined as the expected life time where it remains fully functional without any major rehabilitation (Sohanghpurwala, 2006). The functional service life as driven by chloride induced corrosion of bridge deck reinforcement can be divided into three time periods. First is the initiation time (T_o) which is associated with the duration of period for CO_2 or Cl^- ions to diffuse to the steel-concrete inter-face and activate corrosion reactions. Second one is the expansion time (T_{free}), which is the duration expressed by the period where the corrosion products start expanding and filling the porous zone without resulting pressure build up in the concrete. The third one is the stress build-up time (T_{stress}), which can be defined as the time starting from the beginning of stress development up to the first crack occurs when the build stress is greater than the tensile strength of the concrete. A schematic diagram of the service life model is presented in Fig. 1.

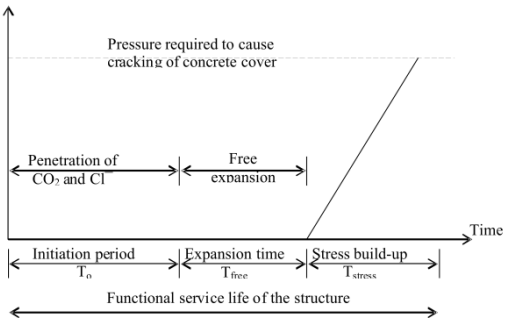

Fig. 1 : Service life model of reinforced concrete structure

The determination of initiation time (T_i) which is represented as the initiation period can be determined by using Fick's second law of diffusion from the diffusivity of the concrete (Miki 1990). A brief review of the models developed by earlier researchers to predict the service life of the reinforced concrete structure is presented in the next section.

2. Review of Models

There are several ways of predicting service life due to the corrosion damage of reinforcement in concrete using different deterioration models. Some of the models reviewed here are presented in detail below.

1. Cady-Weyers' Deterioration Model

Based on the premise that salt-induced corrosion of the steel is the main cause of deck deterioration, a deterioration model developed by Cady and Weyers, 1979 has been used to estimate the remaining life of concrete bridge components in corrosive environments. The model predicts deck deterioration as measured in an area percentage of the entire deck. The total area of spalls, delaminations, asphalt patches, and crack lengths multiplied by a tributary width combine to produce the total damage. There are three distinct phases in the model: diffusion, corrosion and deterioration. The first phase, diffusion, is defined as the time for chloride ions to penetrate the concrete cover and to initiate corrosion. The diffusion time usually can be determined empirically using Fick's Second Law. The second phase, corrosion, is defined as a period of time from initiation of corrosion to first cracking of concrete cover, the time to cracking ranges between 2 to 5 years. The third phase, deterioration, describes the time for damage to reach a level of percent damage which is deemed as the right time for repair or

rehabilitation. According to Cady-Weyers' model, the corrosion rate is the key to predicting the time to cracking. The corrosion rate is largely controlled by the rate of oxygen diffusion to the cathode, resistivity of the pore solution, and temperature.

2. Bazant's Mathematical Models for Time to Cracking

Based on theoretical physical models for corrosion of steel in concrete exposed to seawater, Bazant, 1998 suggested a simplified mathematical model to calculate the time to corrosion cracking of concrete cover. The basic assumptions of Bazant's models are as following:

a. Oxygen and chloride ion transport through concrete cover are quasi-stationary and one dimensional.
b. A steady-state of corrosion producing expansive rust layer begins at depassivation time.
c. The model is based on red rust which is more dangerous for cracking concrete and assumes $\rho_r = \rho_{rt}/4$, where ρ_r and ρ_{rt} are the density of rust products and steel, respectively.

The time of corrosion to cracking, t_{cr}, follows:

$$t_{cr} = \rho_{cor} \frac{D \Delta D}{S j_r} \quad (1)$$

where S is the bar spacing, D is the diameter of the bar, ΔD is the change in diameter of the bar, j_r is the rate of rust production, and ρ_{cor} is a function of the mass densities of steel and rust, $\rho_{cor} = [(1/\rho_r) - (0.523/\rho_{st})]^{-1}\pi/2$.

Stress and cracking caused in concrete cover by this increase in diameter can be routinely solved by a finite element method. Considering concrete to be a homogenous elastic material ΔD, is calculated according to the different failure mode depending on the cover depth and spacing of the reinforcement. If the spacing, S is less than 6D, then the following formula governs ΔD:

$$\Delta D = 2 f_t \frac{L}{D} \delta_{pp} \quad (2)$$

where f_t is the tensile strength of the concrete and δ_{pp} is the bar hole flexibility. For this condition, the expected mode of failure is inclined cracking. The bar hole flexibility is taken as the average of the following bar hole flexibilities, the first being for the case of concrete acting as a thick-walled cylinder and the second being for the case of the concrete acting as an infinite medium:

$$\delta^0_{pp} = \frac{D}{E_{ef}} (1 + \vartheta) + \frac{2D^3}{S^2 E_{ef}} \quad (3)$$

$$\delta'_{pp} = \frac{D}{E_{ef}} \left[1 + \vartheta + \frac{2D^2}{2L(L+D)}\right] + \frac{2D^3}{S^2 E_{ef}} \quad (4)$$

The average of the above two equations, the bar hole flexibility δ_{pp} becomes:

$$\delta_{pp} = \left(\frac{D(1+\varphi_{cr})}{E}\right) \left\{1 + \vartheta + D^2 \left[\frac{2}{S^2} + \frac{1}{4L(l-D)}\right]\right\} \quad (5)$$

where φ_{cr} is the creep coefficient of the concrete , is the Poisson's ratio of the concrete, and *E* is the elastic modulus of the concrete.

If L > (S - D)/2, then another failure mode (cover peeling) governs ΔD :

The time to cracking tcr may be solved from equation (1) if DD is estimated from equation (2)

According to Bazant's models, the time to cracking is a function of corrosion rate, cover depth, spacing, and certain mechanical properties of concrete such as tensile strength, modulus of elasticity, Poisson's ratio and creep coefficient. A sensitivity analysis of Bazant's theoretical equations demonstrates that for these parameters, corrosion rate is the most significant parameter in determining the time to cracking of the cover concrete. Unfortunately, Bazant's model has never been validated experimentally.

3. Morinaga's Empirical Equations

Based on field and laboratory data, the empirical equations suggested by Morinaga, 1988 can be used for predicting the time to cracking. It is assumed that cracking of concrete will first occur when there is a certain quantity of corrosion products forming on the reinforcement. The amount is given by:

$$Q_{cr} = 0.602d \left(1 + \frac{2c}{d}\right)^{0.85} \quad (6)$$

where *Q*cr is the critical mass of corrosion products (10^{-4}g/cm^2);

c is the cover to the reinforcement (mm);

d is the diameter of reinforcing bars (mm).

The time for cracking to take place is given by:

$$t_{cr} = \frac{Q_{cr}}{i_{cor}} \quad (7)$$

where *i*cor is the corrosion rate in gram per day ,*t*cr is the time to cracking in days. The corrosion rate *i*cor can be either measured or estimated statistically from the existing data. According to Morinaga's equations, the time to cracking is a function of the corrosion rate, concrete cover depth and reinforcing size. Therefore, the time to cracking can be easily predicted.

4. Empirical model by Maaddawy and Soudki

As per the model, determination of time from corrosion initiation to corrosion cracking (T_{cor}) can be defined as the time in which the stress builds-up as corrosion products having filled the porous zone. The expansive corrosion products create tensile stresses on the concrete surrounding the corroding steel reinforcing bar. This can lead to cracking and spalling of concrete cover as a usual consequence of corrosion of steel in concrete.

The empirical model proposed by Maaddawy and Soudki, 2007 has been chosen here for predicting the time to corrosion cracking of the concrete because of the simple mathematical approach. This model simply relates the steel mass loss and the internal radial pressure caused by the expansion of corrosion products developed. The concrete around a corroding steel reinforcing bar is modeled as a thick-walled cylinder with a wall thickness equal to thinnest concrete cover. The concrete ring is assumed to crack when the tensile stresses in the circumferential direction at every part of the ring have reached the tensile strength of concrete. The internal radial pressure at cracking is then determined and related to steel mass. With the help of Faraday's law the time from corrosion initiation to corrosion cracking is then predicted. These are two important equations presented here from the model paper.

$$P_{cor} = \frac{2M_{loss}E_{ef}\left(0.622\rho_r - \rho_s\right)}{\pi D\left(\nu+\varphi\right)\left(D+2\delta_0\right)} - \frac{2\delta_0 E_{ef}}{\left(\nu+\varphi\right)\left(D+2\delta_0\right)} \quad (8)$$

$$T_{cr} = \left[\frac{7117.5\left(D+2\delta_0\right)\left(\nu+\varphi\right)}{iE_{ef}}\right]\left[\frac{2Cf_{ct}}{D} + \frac{2\delta_0 E_{ef}}{\left(\nu+\varphi\right)\left(D+2\delta_0\right)}\right] \quad (9)$$

Where,

C = clear concrete cover (mm)

D = diameter of steel reinforcing bar (mm)

E_{ef} = effective elastic modulus of concrete

f_{ct} = tensile strength of concrete

I = current density

P_{cor} = internal radial pressure caused by corrosion

T_{cr} = time from corrosion initiation to corrosion cracking

M_{loss} = mass of steel per unit length consumed to produce M_r

M_r = mass of rust per unit length

δ_0 = thickness of porous zone

ν = Poisson's ratio (0.18 for concrete)

ρ_s = mass density of steel

ρ_r = mass density of rust

ψ = factor depends on D, C and δ_0

Porous zone thickness is an important parameter for determining the time from corrosion initiation to corrosion cracking. It is observed from the literature that the typical range of the porous zone thickness varies from 10µm to 20µm (Christensen, T. P. 2000) and 30 µm-60 µm (Yuan and Y Ji, 2009). The corrosion cracking model proposed by Maadawy and Sudoky takes corrosion current density as one of the input. A typical plot showing the corrosion current density and the corrosion cracking time is presented in Fig. 2. It can be observed from the Fig. that the time to corrosion cracking is inversely proportional to the corrosion current density. Further the unit conversion from corrosion current density to corrosion rate table is presented in Table 1. It is necessary to present the graph in corrosion rate versus the time to corrosion cracking. Hence all the units of the corrosion current density is converted to corrosion rate by following the unit conversion Table 1 and the plot between corrosion rate against the corrosion cracking time is presented in Fig. 3. It can be observed from the figure that the time to corrosion cracking is inversely proportional to the corrosion rate. It is to be noted that by knowing the corrosion rate of steel in any structure, the time from corrosion initiation to corrosion cracking can be simply determined from Fig. 3.

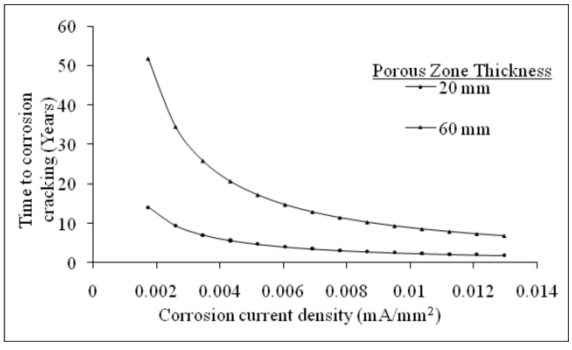

Fig. 2: Relationship between corrosion current density and time to corrosion cracking

Table 1 : Unit converstion from corrosion rate to corrosion current density

	mA cm^{-2}	mm year^{-1}	mpy	g m^{-2} day^{-1}
mA cm^{-2}	1	11.6	456	249
mm year^{-1}	0.0863	1	39.4	21.6
mpy*	0.00219	0.0254	1	0.547
g m^{-2} day^{-1}	0.00401	0.0463	1.83	1
* mpy = milli-inch per year				

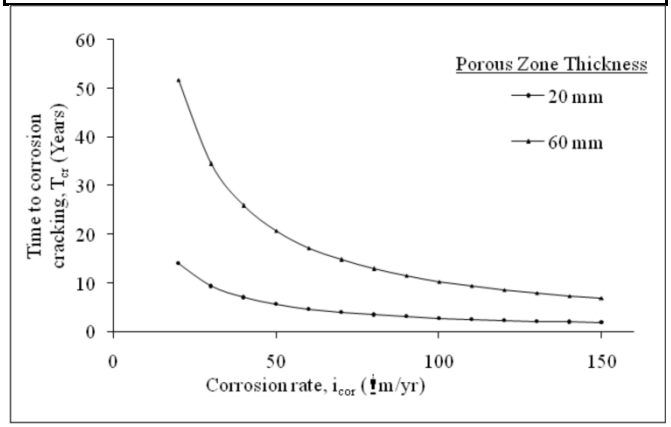

Fig. 3 : Relationship between corrosion rate (i_{cor}) and time to corrosion cracking (T_{cr})

Correlation between Corrosion Rate and Half-Cell Potential

The model adopted in this research investigation need the corrosion rate (µm/year) as the one of the important input in determining the corrosion cracking time (T_{cor}). However, accurately determining the corrosion rate of the steel reinforcement in the bridge is not always possible because of a number of other reasons. On the other hand, measuring the corrosion potential by employing the corrosion analyzing instrument (CANIN) is well established and it is being adopted a handy tool for the field engineers and the maintenance personals. Based on this concept a relationship between the corrosion rate (µm/year) data and the half-cell potential (-mV) data is being given by previous researchers (Kibraeb A Gebreselassie, 2011) is considered in this study and is plotted in Fig. -4. It can be observed from the figure that a power relationship between the half-cell potential and corrosion rate with a correlation coefficient of 0.97 exist. By using this correlation all the half cell potential data (measured by CANIN) of the field investigated bridges were converted to corrosion rate which was later used to estimate the functional service life.

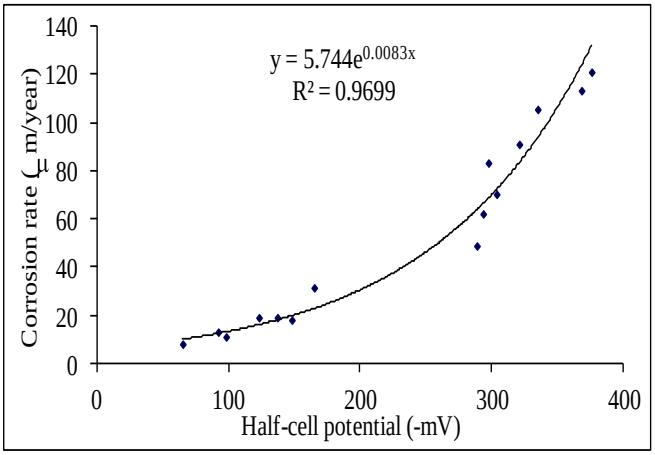

Fig. 4 : Correlation between half cell potential and corrosion rate

Table -2 : A sample copy showing the calculation steps of time required from corrosion initiation to corrosion cracking

PARAMETERS	VALUE
Internal Radius of the Cylinder (a), mm	8.02
Effective Elastic modulus of a thick walled cylinder (E_{ef}), Mpa	2900
Exterior Radius of the cylinder (b), mm	46.02
Poisson's Ratio(ν)	0.20
Internal Radial Pressure (P)	
Diameter of the Steel Reinforcing Bar(D), mm	16
Thickness of the porous Zone (δ_0), mm	0.02
Total Diameter of the Steel reinforcing (D'), mm	16.04
Wall Thickness of the Cylinder C, mm	38
Reconsidered (a), mm	8.02
Reconsidered (b), mm	46.02
Considering ψ	0.06
Mass of Rust per unit length of bar (M_r), kg/mm	0.0013
Ratio of Molecular Mass of Steel to molecular mass of rust (γ)	0.622
Mass density of Rust (ρ_r), kg/m^3	5240
Mass Density of steel (ρ_s), kg/m3	7850
Percentage Steel Mass Loss (m_1)	53.42
Concrete Tensile Strength (f_{ct}), Mpa	5.17
Current Density (i), mA/mm^2	0.04
Time from corrosion initiation to corrosion cracking(T_{cr}), Years	0.84
Time from corrosion initiation to corrosion cracking(T_{cr}), Days	308

Case Study on Panvel Creek Bridge

Panvel creek bridge serves as the main access from Belapur, Navi Mumbai to Jawaharlal Nehru Port Trust, Uran. It takes the load of medium and heavy traffic with majority of container load vehicles are plying throughout. The bridge is 40 years old, having total length of 397.00 meters, and width of 13.10 meters. It has 9.50 meters carriageways and 1.8 meter footpath on either side. The bridge is rest on support of circular pier with pile foundation. There is a 3.5 to 4.0 meter difference between high tide level and low tide levels (the splash zone) due to which piers have been affected to a large extent. It has been observed that the foundation of the reinforced concrete structure is constantly exposed to the saline water. A line diagram is presented in Figure 5.

Prediction of Remaining Life Service of Panvel Bridge-Case Study

The remaining service life of the bridge structure is determined by considering the average half-cell potential value measured and presented in Table 3. Further detail investigation carried out on this bridge is reported somewhere else (Godbole et. al., 2014).

Based on the average value of half-cell potential value measured in the year May-2013, the remaining service life of the structure is determined as per the procedure explained above and listed in Table 4.

Considering the half-cell potential data reported in the above table and the calculated remaining service life, it can be understood that the bridge is at the critical stage of deterioration. Based on the developed service life model, the remaining service life is only from 6-9 years for all the components of the bridge. This needs an immediate care and maintenance strategy of rehabilitation.

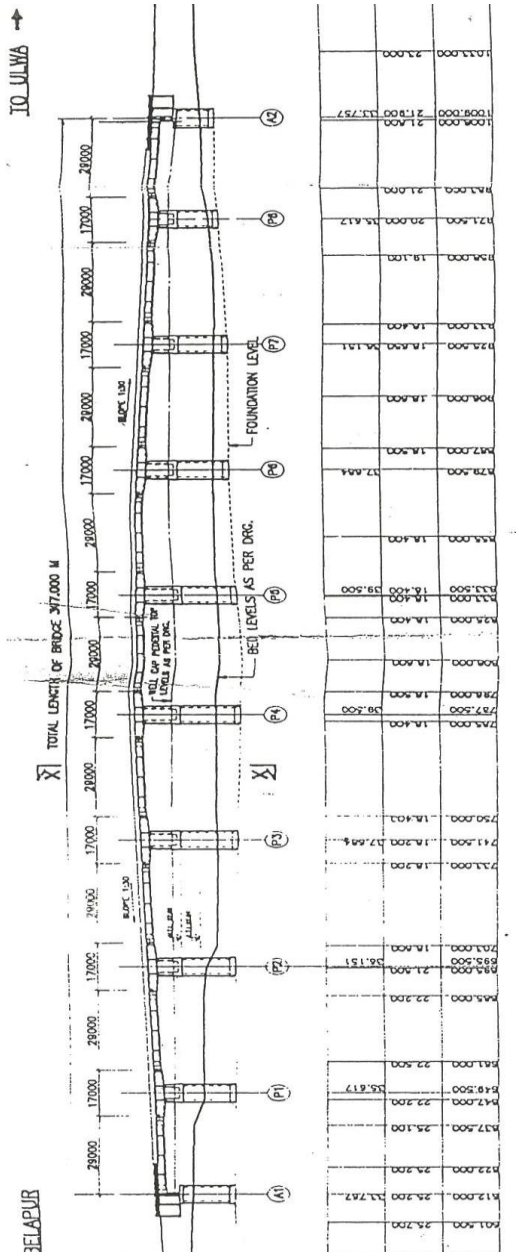

Fig 5.Panvelcreek bridge elevation and plan

When contacted to the concerned authority responsible for the maintenance of the bridge, it is understood that the vehicular traffic on this bridge completely stopped and diverted on the newly constructed bridge. The rehabilitation of the bridge work is in under planning to get major repairs of piers, cross beams and deck slab of the bridge. The field test conducted on the bridge component for the academic research study which reveals the probability of corrosion condition for establishing the remaining life service of the structures.

Table 3 : Bridge Case Study Data of Half Cell Potentiometer Test (2013)

ID. MARK	Observation (mV)								Average (mV)
Beam Betn. Pier No.P3 and P4	-415	-430	-415	-430	-415	-430	-440	-435	**-427**
	-430	-425	-435	-430	-440	-440	-430	-435	
	-405	-415	-420	-435					
Slab Betn. Pier No.P3, P4, P5 and P6	-430	-435	-430	-420	-425	-420	-430	-425	**-431**
	-435	-440	-425	-430	-425	-440	-435	-440	
	-430	-445	-440	-430					
Beam Betn. Pier P4 and P5	-415	-420	-425	-410	-425	-440	-410	-415	**-413**
	-390	-415	-410	-425	-395	-405	-395	-418	
	-440	-415	-390	-400					
Beam Betn. Pier No.P5 and P6	-415	-420	-435	-415	-420	-425	-435	-440	**-427**
	-430	-425	-420	-445	-435	-430	-405	-422	
	-430	-435	-420	-440					
Slab Betn. Pier No.P4, P5, P6 and P7	-395	-405	-420	-425	-420	-380	-405	-420	**-417**
	-415	-415	-415	-405	-430	-435	-440	-420	
	-395	-420	-435	-440					
Pier No.P4	-400	-405	-420	-435	-440	-440	-390	-395	**-418**
	-430	-435	-410	-405	-415	-425	-430	-400	
	-405	-420	-425	-440					
Pier No. P5	-375	-360	-375	-390	-385	-370	-360	-370	**-378**
	-390	-375	-370	-390	-400	-360	-375	-380	
	-382	-378	-390	-392					
Pier No. P6	-380	-360	-390	-400	-405	-375	-360	-390	**-384**
	-400	-380	-315	-405	-395	-330	-415	-400	
	-415	-365	-405	-400					

Table 4 : Service life estimation of different components of the bridge

Sl. No	Location	Average half-cell potential value (mv)	Remaining Service life (years)
1	Beam between pier no. P3 and P4	-427	6.0
2	Beam between pier no. P4 and P5	-413	6.7
3	Beam between pier no. P5 and P6	-427	6.0
4	Slab between pier no. P3, P4, P5 and P6	-431	6.0
5	Slab between pier no. P4, P5, P6 and P7	-417	6.6
6	Pier no. P4	-418	6.6
7	Pier no. P5	-378	9.0
8	Pier no. P6	-384	8.5

Validation of Model for Other Structures

1. Name of the Project / Site Rehabilitation of Minor Bridge near Wahal village on Belapur Uran road at Ulwe Node, Navi Mumbai. Test method followed, if any ASTM/C876-80 Date of Testing 23/03/2006

Table 5 : Report of Half Cell Potentiometer Test on Minor Bridge near Wahal Village

ID. MARK	Observation (mV)								Average (mV)
Beam between Pier No.B1 and B2	-395	-410	-412	-420	-410	-402	-405	-410	
	-412	-408	-410	-408	-415	-420	-410	-412	-407
	-390	-388	-390	-405					
Slab between Pier No.B1, C1, B2 and C2	-420	-430	-428	-415	-420	-410	-425	-415	
	-420	-432	-390	-410	-410	-425	-420	-415	-419
	-420	-440	-430	-410					
Beam between Pier C2 and D2	-388	-400	-395	-370	-388	-395	-380	-390	
	-365	-390	-400	-420	-365	-390	-365	-410	-419
	-415	-380	-375	-388					
Pier No.C4	-380	-375	-380	-402	-412	-398	-360	-400	
	-410	-415	-400	-390	-395	-390	-400	-372	-394
	-388	-400	-405	-410					
Beam between Pier No.C4 and D4	-440	-410	-415	-408	-410	-410	-420	-412	
	-420	-412	-420	-432	-420	-395	-400	-415	-415
	-425	-410	-410	-415					
Slab between Pier No.C4, C5, D4 and D5	-360	-400	-410	-415	-400	-345	-390	-408	
	-400	-410	-385	-400	-412	-410	-415	-390	-395
	-372	-388	-390	-395					

Based on the half-cell potential data reported in the Table 5 it can be understood that the bridge is at the critical stage of deterioration. Based on the developed service life model, the remaining service life is merely 5 years for all the components of the bridge. This needs an immediate care and maintenance strategy of rehabilitation.

It is found that, government agencies immediately decided not to use the bridge. In spite of going for a major rehabilitation which was necessary at that point in 2006, the major traffic has been diverted to another route to avoid any kind of mishap. The bridge presently uses only the light vehicles. This validates the service model is working perfectly alright for the bridge structure.

Table 6 : Results of Half Cell Potentiometer Test Data conducted at Vasani Chamber

Sr. No.	Level	Location	Average Half Cell Potential (mv)
1.	G-1	C42	-396
2.	G-1	C43	-392
3.	G-1	C44	-270
4.	G-1	C45	-390
5.	G-1	C46	-309
6.	G-1	C49	-315
7.	G-1	C51	-381
8.	G-1	C52	-298
9.	G-1	C53	-389
10.	G-1	C54	-371
11.	G-1	C55	-345
12.	G-1	C56	-391
13.	G-1	C68	-284
14.	G-1	C42	-258
15.	G-1	C43	-215
16.	G-1	C44	-300
17.	G-1	C45	-281
18.	G-1	C46	-286
19.	G-1	C49	-274

2. Name of the Building: VASHANI CHAMBER
Address : 47, Sir Vithaldas Thackersey Marg,
New Marine Lines, Mumbai – 400 020
Date of inspection and Tests: 1st to 6th September, 2014
Year of Construction : Around 1903- Ground floor (G + 5)
Mode of use a) Original use : Residential cum Commercial
b) Present use : Commercial (offices)

Type of building: Ground plus mezzanine plus Five upper storied composite structures.

The data of half cell potential study conducted is presented in Table 6. Based on the data of the half-cell potentiometer study conducted, the remaining service life of the structure is determined from the service life model as 6 years as per the largest value measured at the location "C42". However, considering the average value of the half-cell potential reading for the whole structure is concerned, the remaining service life of the structure is determined to be 10 years. It is to be noted that the a maintenance plan need to be strategically developed at the end of six years of time and the same may vary from 6 years to 10 years of time, considering the rate of deterioration at the present instant remains constant for the rest of the life of the structure.

The structural audit report indicates that the whole building structure is not in dilapidated condition, which is validating the result from the model. However, at present the building structure is not in a habitable condition. To avoid any loss of life, the building is already vacated for rehabilitation work.

3. Name of the Project / Site: Turbhe Flyover on Sion - Panvel Road Navi Mumbai Test method followed, if any: ASTM/C876-80 Date of Testing: 07/06/2005 to 16/06/2005- The half-cell data is presented in Table 7.

Table 7 : Report of Half Cell Potentiometer Testing

ID. MARK	**Half-cell Potentiometer Data (mV)**								**Average (mV)**
Mumbai - Panvel Arm									
Span A1 - P1	-230	-231	-245	-249	-253	-256	-286		
LWD - 3	-287	-291	-289	-265	-286	-288	-296		-272
Internal Web	-299	-300	-288	-265	-267	-268			
Span P1 - P2	-198	-220	-225	-199	-174	-225	-228		
RWD - 1	-235	-199	-238	-241	-245	-256	-268		-239
Internal Web	-267	-278	-225	-287	-286	-287			
Span P2 - P3	-286	-285	-287	-288	-289	-289	-284		
LWD - 1	-280	-274	-268	-274	-268	-225	-220		-251
Internal Web	-218	-196	-175	-189	-220	-211			
Span P3 - P4	-218	-220	-221	-221	-218	-217	-215		
RWD - 1	-199	-204	-225	-206	-218	-220	-235		-231
Internal Web	-240	-254	-262	-287	-280	-267			
Span P5 - P6	-219	-225	-224	-226	-228	-237	-240		
RWD - 1	-245	-250	-256	-258	-260	-265	-267		-241
Internal Web	-220	-222	-223	-229	-235	-286			
Span P6 - P7	-245	-248	-249	-250	-256	-258	-247		
LWD - 1	-248	-286	-289	-258	-260	-264	-266		-262
Internal Web	-262	-260	-250	-274	-276	-284			
Span P11 - P12	-230	-232	-280	-282	-290	-300	-312		
RWD-2	-328	-320	-310	-305	-299	-288	-312		-290
	-301	-289	-281	-285	-280	-278			
Span P12 - P13	-220	-218	-216	-200	-212	-212	-198		
From External Web	-200	-215	-214	-216	-220	-221	-220		-213
East Face	-225	-230	-218	-206	-204	-199			
Span P13 - P14	-198	-174	-188	-165	-168	-175	-199		
From External Web	-200	-205	-199	-197	-178	-168	-177		-187
East Face	-186	-189	-192	-198	-195	-179			
Span P14 - A4	-225	-230	-228	-222	-220	-198	-240		
From External Web	-238	-230	-228	-226	-224	-218	-206		-187
East Face	-215	-214	-210	-211	-212	-230			
Span P14 - A4	-198	-220	-225	-213	-199	-200	-183		
D-2 (Diaphragm)	-223	-228	-235	-235	-251	-248	-250		-221
	-253	-230	-218	-227	-226	-231			

Based on the data presented in the above Table, the remaining service life of the flyover is determined considering the highest and lowest value of the half-cell potential value. It is to be noted that the Flyover has a remaining service life of 34 years considering the lowest value of the half-cell potential data. However, some component of the structure is exposed to very severe environments and deteriorated at a faster rate than other part. It is to be noted that for most part of the structure the maintenance program will be needed at the end of 34 years, however, the internal and external web, where the half-cell potential reading is relatively high need a maintenance program at the end of 10 years.

It is found that in the year 2012-13 (at the end of 8 years after the non-destructive testing), a minor repair work such as crack opening and filling with high strength mortar, grouting and epoxy painting at external and internal surface of concrete girder, piers, bottom deck slab was already carried out. This is justifying the model's authenticity in actually determining the remaining service life of the structure and also validating it.

Conclusions

Half cell potentiometer data are quite useful to to establish remaining life service of reinforced concrete structures. The life service model proposed by Maadawi and Sudoki to predict the end of service function of structures is working perfectly and can be strategically employed to rehabilitee major repairs so that any kind of total loss of life and resources can be avoided.

References

[1] Bazant ZP. Physical model for steel corrosion in concrete sea structures-applications. J Struct Div 1979 (June):1155-65.

[2] Cady and Weyers RE. Service life model for concrete structures in chlorideladen environments. ACI Mater J 1998;95 (4):445–53.

[3] Christensen, T. P. (2000), "Stochastic Modelling of the Crack Initiation Time for Reinforced Concrete Structures". ASCE Structures Congress, Philadelphia, pp. 8.

[4] Godbole K.M., Dr. P.H. Sawant and Dr. B.B. Das, Advanced Research in Civil and Environmental Engineer (JOARCEE) "Corrosion Assessment Of Reinforced Steel Bars In Concrete Structures Exposed to Under Marine Environment. - Bridge Case Study." ISSN : 2393-8307 J.Adv. Res. Civil Env. Eng.2014; Vol.1 (3and4): 1-16.

[5] Kibraeb A Gebreselassie, "Effects of freeze-thaw and salt-water exposure on the corrosive environment in bridge decks", Thesis (M.S. Civil Eng.)--Lawrence Technological University, 2011.

[6] Maaddawy TE, Soudki K., "A Model for prediction of time from corrosion initiation to corrosion cracking", Cement and Concrete composites 29 (2003) 168-175.

[7] Miki, F., (1990). "Predicting Corrosion-free Service Life of a Concrete Structure in a Chloride Environment", ACl Materials Journal, Vol. 87 (6), pp. 581-587.

[8] Morinaga S. Prediction of service lives of reinforced concrete buildings based on rate of corrosion of

reinforcing steel. Report No. 23, Shimizu Corp, Japan; 1988. p. 82.

[9] Sohanghpurwala, A. A. (2006). "Service Life of Corrosion Damaged Reinforced Concrete Bridge Superstructure Elements", NCHRP report 558, Transportation Research Board, Washington DC.

[10] Weyers RE. Service life model for concrete structures in chloride laden environments. ACI Mater J 1998;95 (4):445–53.

[11] Yuan, Y., and Ji, Y. (2009). "Modeling Corroded Section Configuration of Steel Bar in Concrete Structure", Construction and Building Materials, Vol. 23, pp. 2461–2466.